

A review of the main results about the Venus' atmosphere from VIRTIS on Venus Express. G. Piccioni¹, P. Drossart², and the VIRTIS-Venus Express team, ¹IASF-INAF (Rome, Italy, via del Fosso del Cavaliere, 100, 00133 Roma, giuseppe.piccioni@iasf-roma.inaf.it), ²Obs de Paris-Meudon (Meudon, 5, Place J. Janssen, 92195, Meudon - France, pierre.drossart@obspm.fr).

Introduction: After about 3 years from the Venus orbit insertion, the Visible and InfraRed Thermal Imaging Spectrometer (VIRTIS) [1,2] on board the ESA Venus Express mission provided, and is currently providing, an extended data set very valuable to study Venus from the surface up to the thermosphere in long term.

The VIRTIS instrument consists of two channels: VIRTIS-M, an imaging spectrometer with moderate spectral resolution in the range from 0.25 to 5 μm and VIRTIS-H, a high spectral resolution spectrometer in the range from 2 to 5 μm co-aligned with the field of view of -M. The spectral sampling of VIRTIS-M is 2 nm from 0.25 to 1 μm and 10 nm from 1 to 5 μm while for VIRTIS-H it is about 2 nm.

Atmospheric Composition: Radiance originating in the deep atmosphere and escaping in the atmospheric windows has been used to infer the chemical composition in the dark side of the planet below the clouds. In particular, the window in the region at about 2.3 μm is effective to retrieve the abundance of CO, H₂O, OCS and SO₂ at about 30-35 km altitude [3,4]. CO, which is considered a tracer of the global dynamics, is typically found to be in the range 25-30 ppm with significant meridional gradient with a maximum at about 60° latitude. OCS results to be anticorrelated with CO and its abundance is in the range 2.5-4 ppm. H₂O and SO₂ are found to be relatively more spatially homogeneous with an abundance around 30 and 130 ppm respectively. In the illuminated side of the planet, the solar reflected light from the clouds top can be used to retrieve the mesospheric composition. In particular, water vapour is typically found to be around 5 ppm but with some variability.

Dynamics and Clouds Morphology: Clouds tracking has been used to measure the winds speed [5]. Measurements at different altitude level are possible by using the UV and IR solar reflected radiances at 350 nm and 980 nm in the day side, see Fig.1. These two wavelengths probe the altitude level at about 65 and 61 km altitude respectively. Additionally, in the night side of the planet, the radiance in the window at 1.74 μm provides the way to measure winds in the lower clouds at about 47 km altitude. The winds speed shows a significant vertical shear at low latitudes with values from about -50, -70 and -110 m/s in the 3 probed layers, with a speed relatively constant poleward up to about -60°S where the vertical shear disap-

peared in combination with a decreasing speed toward the pole.

The polar vortex dominates the dynamics in the polar region with a rich amount of details and enhanced contrast. It has been observed in a dipole configuration right at the beginning of the mission [6]. The dipole-like shape was similarly observed in the north by the past Pioneer Venus mission and thus it seemed to be a stable feature. However, in the course of the Venus Express mission, a large number of different shapes of the vortex have been observed, from single mode to mode 3 or even more complex configurations with a not well identified stable feature, see Fig.2.

The clouds morphology shows different dynamical regimes. At low latitudes is visible a significant convection on both day (at an altitude of about 65-70 km) and night (at an altitude of about 45-50 km) sides of the planet. The former fed by the strong solar heating on the clouds top, while the latter excited by the strong thermal radiation coming from the surface or the deep atmosphere below the clouds. The mid-latitudes show a more regular streaky clouds, very elongated and less turbulent. Toward the pole the clouds tend to be more spiraling and in close connection with the vortex structure.

Significant waves activity have been observed from the lower clouds up to the upper mesosphere with no apparent correlation with surface and absence of recurrent spatially localized features.

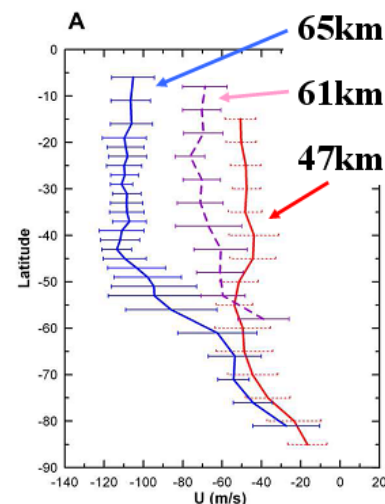


Figure 1: Winds speed from clouds tracking.



Figure 2: The polar vortex at $3.8 \mu\text{m}$, probing on the clouds top. The shape here is circular. The darker region corresponds to higher temperature and lower altitude.

Temperature structure: The atmospheric temperature structure in the night side of Venus has been retrieved from the CO_2 absorption band at $4.3 \mu\text{m}$, in the pressure range 100 - 0.1 mbar, corresponding to about 65 - 90 km altitude respectively [7]. The temperature typically increases toward the pole in the entire altitude range effectively sounded by VIRTIS. An exception exists at the approximate level of the clouds top altitude - about 65-70 km - where a local cold minimum around $60\text{-}70^\circ\text{S}$ is observed. This is the cold collar region and it is also a region of strong thermal inversion. In terms of variability, fluctuations are observed both on short and long time scales, especially around 1 mbar. The highest temperature contrast is seen in the lowest layer effectively probed at about 65-70 km altitude where both cold collar and polar vortex dominate the dynamics from mid-to-high latitudes. At this altitude, the temperature is in average warmer at dusk than at dawn and the most important gradient, about 10K, is observed around 70°S , again in the cold collar region. This thermal contrast tends to vanish at higher altitudes where the atmosphere becomes more horizontally isothermal.

Nightglows and CO_2 Non-LTE effects: The oxygen nightglow is a very important mean to study the dynamics and chemistry of the upper atmosphere. The most intense nightglow emission is observed at $1.27 \mu\text{m}$ and it is due to the (0-0) transition [8,9]. Both limb and nadir views provide the 3-dimensional structure of the emission, see Fig.3. The peak altitude of the limb profile is typically found at 96-97 km, with a maximum emission at low latitudes and near the antisolar point. The nadir measurements confirm the same behaviour and the global mean map of the oxygen night-

glow shows an almost perfect symmetry of the SS to AS circulation, with a maximum of the emission rate in the antisolar region of about 1.2 MR. The apparent motion of the tracked emission features show very complex but with a sign of a mean zonal speed of about + 50 m/s, and thus opposite to the atmospheric super-rotation [10].

The hydroxyl nightglow has been recently discovered on Venus at 2.8 (1-0 transition) and $1.46 (2\text{-}0 \text{ transition}) \mu\text{m}$ [11]. It peaks a couple of km lower than the oxygen. The most probable mechanism is the Bates-Nicolet from the combination of H and O_3 . OH nightglow is thus an important tool to infer the abundance of these two chemical species.

More recently, the NO infrared nightglow emission at $1.224 \mu\text{m}$ has been observed for the first time in the VIRTIS spectra [12]. The NO nightglow typically peaks at about 110 km altitude.

CO_2 fluorescence at 2.7 and $4.3 \mu\text{m}$ has also been observed and studied in the day side of the planet and compared with the models. The emitting layers are placed in a range of altitudes from 100 to 140 km.

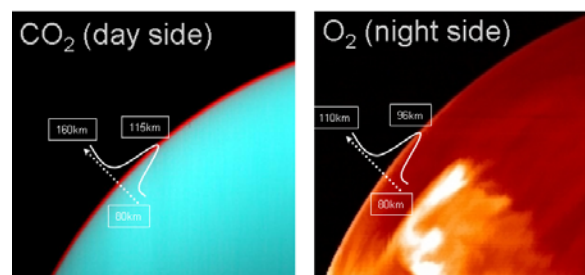


Figure 3: CO_2 fluorescence on the day side at $4.3 \mu\text{m}$ (left) and oxygen nightglow at $1.27 \mu\text{m}$ (right).

References: [1] Piccioni G., et al., (2008), ESA-SP, in press. [2] Drossart P., et al., (2007), *Planetary and Space Science* 55(12), 1653—1672. [3] Marcq E., et al., (2008), *JGR*, in press. [4] Tsang, C., et al., (2008), *JGR*, in press. [5] Sanchez-Lavega, A., et al. (2008), *Geophysical Research Letters* 35(13). [6] Piccioni G., et al. (2007), *nature*, 450, 637-640, 2007. [7] Grassi D. et al. (2008), *JGR*, in press. [8] Drossart P., et al., (2007), *nature*, 450, 641-645, 2007. [9] Gérard, J.-C., et al., (2008), *Geophysical Research Letters*, VOL. 35, L02207. [10] R. Hueso, et al., (2008), *JGR*, in press. [11] Piccioni G., et al., (2008), *A&A* 483, L29–L33. [12] Garcia Munoz A., et al. (2009), *PNAS*, in press.

Additional Information: We wish to thank ESA, ASI, CNES and the other agencies supporting this program.